AD-A171 082 MEASUREMENT OF SURFACE PRESSURES CAUSED BY A PROJECTILE ROTATING BAND AT..(U) ARMY BALLISTIC RESEARCH LAB ABERDEEN PROVING GROUND MD J E DAMBERG ET AL. JUL 86 BRL-MR-3532 1/1

UNCLASSIFIED F/G 19/1 NL

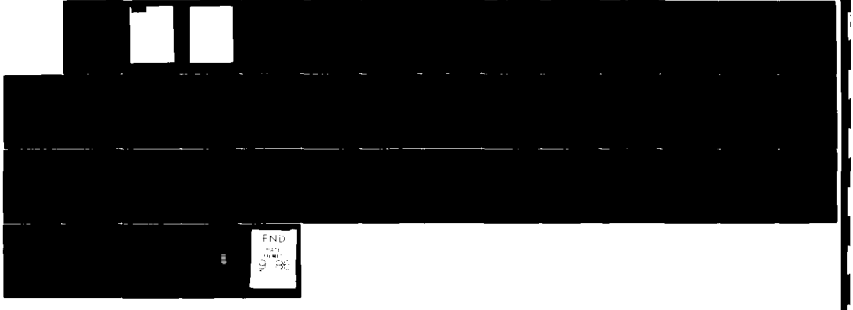

END

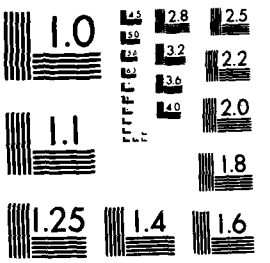

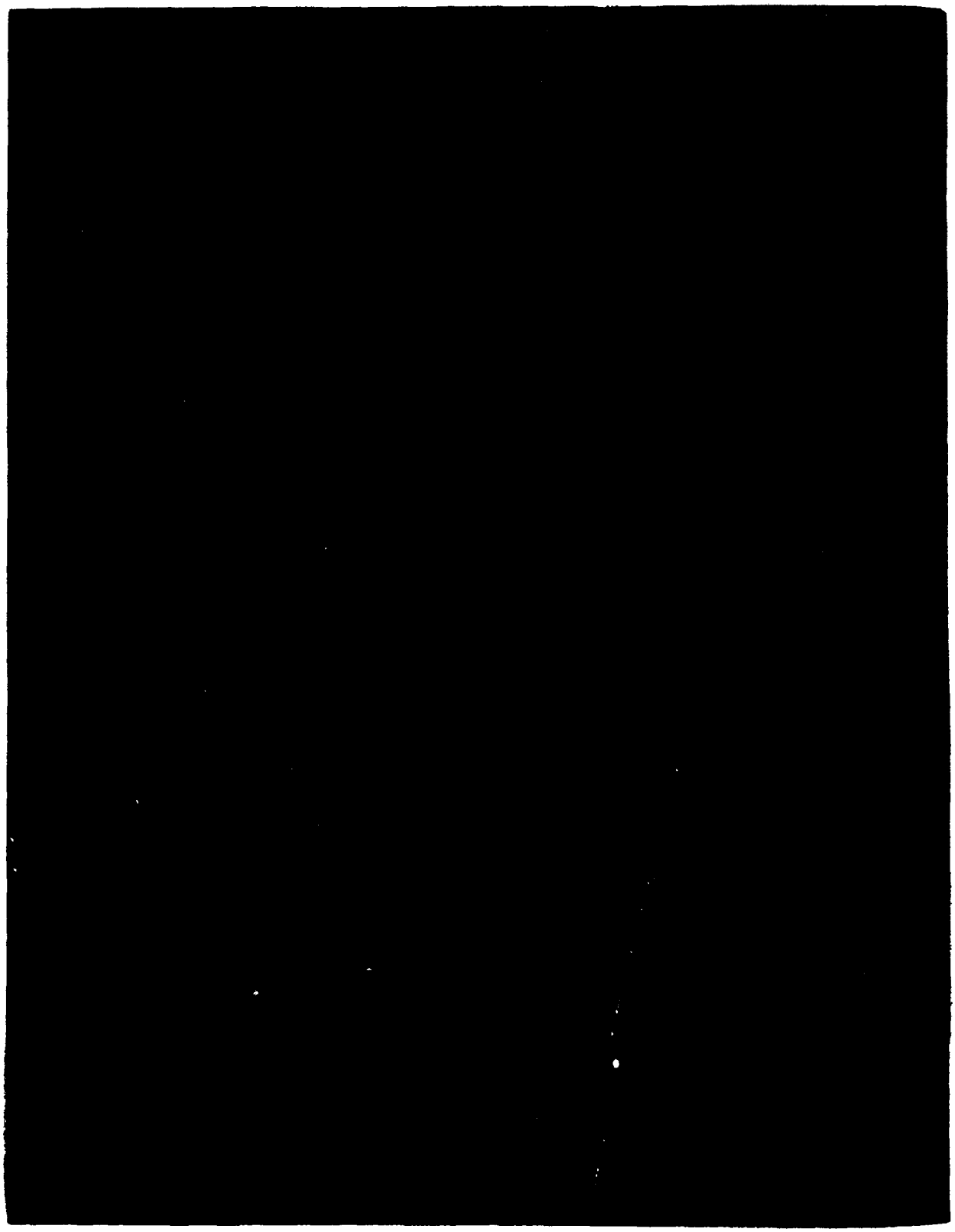

UNCLASSIFIED
SECURITY CLASSIFICATION OF THIS PAGE AD-A171082

REPORT DOCUMENTATION PAGE

Form Approved OMB No 0704-0188 Exp. Date Jun 30, 1986

1a. REPORT SECURITY CLASSIFICATION: UNCLASSIFIED	1b. RESTRICTIVE MARKINGS
2a. SECURITY CLASSIFICATION AUTHORITY	3. DISTRIBUTION/AVAILABILITY OF REPORT: Approved for public release, distribution unlimited.
2b. DECLASSIFICATION/DOWNGRADING SCHEDULE	
4. PERFORMING ORGANIZATION REPORT NUMBER(S): Memorandum Report BRL-MR-3532	5. MONITORING ORGANIZATION REPORT NUMBER(S)
6a. NAME OF PERFORMING ORGANIZATION: U.S. Army Ballistic Research Laboratory; 6b. OFFICE SYMBOL (If applicable): SLCBR-LF	7a. NAME OF MONITORING ORGANIZATION
6c. ADDRESS (City, State, and ZIP Code): Aberdeen Proving Ground, Maryland 21005-5066	7b. ADDRESS (City, State, and ZIP Code)
8a. NAME OF FUNDING/SPONSORING ORGANIZATION; 8b. OFFICE SYMBOL (If applicable)	9. PROCUREMENT INSTRUMENT IDENTIFICATION NUMBER
8c. ADDRESS (City, State, and ZIP Code)	10. SOURCE OF FUNDING NUMBERS

PROGRAM ELEMENT NO.	PROJECT NO.	TASK NO.	WORK UNIT ACCESSION NO
RDT&E	1L162618	AH80	

11. TITLE (Include Security Classification)
MEASUREMENT OF SURFACE PRESSURES CAUSED BY A PROJECTILE ROTATING BAND AT SUPERSONIC SPEEDS

12. PERSONAL AUTHOR(S)
DANBERG, JAMES E. AND PALKO, KEITH L.*

13a. TYPE OF REPORT	13b. TIME COVERED	14. DATE OF REPORT (Year, Month, Day)	15. PAGE COUNT
Final	FROM _____ TO _____	July 1986	42

16. SUPPLEMENTARY NOTATION
* University of Delaware, Mechanical & Aerospace Engineering Dept., Newark, DE 19711

17. COSATI CODES			18. SUBJECT TERMS (Continue on reverse if necessary and identify by block number)
FIELD	GROUP	SUB-GROUP	
01	01		Separated Flow; Projectile Drag; Rotating Band; Pressure Distribution

19. ABSTRACT (Continue on reverse if necessary and identify by block number)

An experiment is described in which surface pressure distributions on a cone-cylinder model have been measured with and without a simulated rotating band. Measurements cover a Mach number range from 2.25 to 3.50 at an average Reynolds number of 1.3 X 10**6. Increased resolution of the pressure distribution was achieved by using a movable band with only five orifices on the constant pressure cylindrical section of the model. The results show that the perturbation pressures caused by the band are independent of the actual band location. A second phase of the experiments concerned measuring the pressure changes caused by various band thicknesses which were produced by wrapping layers of tape around the model.

The pressure disturbance of the band is found to correlate in terms of the maximum and minimum pressure coefficients and pressure interaction lengths. The interaction length ahead of the band is found to be nearly constant and the maximum pressure coefficient is inversely

20. DISTRIBUTION/AVAILABILITY OF ABSTRACT	21. ABSTRACT SECURITY CLASSIFICATION
☒ UNCLASSIFIED/UNLIMITED ☐ SAME AS RPT. ☐ DTIC USERS	UNCLASSIFIED

22a. NAME OF RESPONSIBLE INDIVIDUAL	22b TELEPHONE (Include Area Code)	22c. OFFICE SYMBOL
Dr. James E. Danberg	(301) 278-4280	SLCBR-LF-R

DD FORM 1473, 84 MAR 83 APR edition may be used until exhausted. All other editions are obsolete.

SECURITY CLASSIFICATION OF THIS PAGE UNCLASSIFIED

19. Abstract (Continued)

proportional to $\beta = (M^2-1)^{1/2}$. Behind the band the interaction length increases proportional to β whereas the minimum pressure coefficient is inversely proportional to β^2. The tape band results enabled the correlation formulas to be extended to include the effect of band height.

Correlations of the pressure distributions on the cylinder in front of, and behind the band has lead to estimates of the drag on practical projectile configurations at supersonic Mach numbers.

ACKNOWLEDGEMENT

The authors wish to express their thanks to the staff of the Aerodynamics Research and Concepts Assistance Branch, U.S. Army Chemical Research Development and Engineering Center, Aberdeen Proving Ground, MD, for their help and cooperation in carrying out these experiments in their facility. Special recognition is due Frank G. Wrede, Jr. who set up and calibrated the instrumentation and carried out all the tests.

TABLE OF CONTENTS

LIST OF FIGURES

I. INTRODUCTION

The objective of this report is to describe the results from a series of supersonic wind tunnel tests designed to measure the pressure distribution in front of, as well as behind a ring protuberance (of the order of the boundary layer thickness) on an axisymmetric body. In principle, the construction of such a model is straight forward. However, there are practical limitations on the resolution of the pressure distribution which can be obtained; particularly with small models. In order to increase the detail observed, an attempt has been made here to measure the pressure distribution using a few fixed pressure orifices located in front of and behind a movable band. The band's range of positions are all located in a nearly constant pressure region on the basic model. Therefore, it can be assumed that the boundary layer thickness varies only slightly over the region of the band positions. It was expected that the pressures induced by the protuberance would be effected only in a secondary way by the changing position of the band. Thus it is also an objective of this work to assess the validity of this assumption.

The flow over a protuberance is a fundamental and difficult problem in fluid mechanics. It involves the strong interaction of separated flow regions ahead of and behind the obstacle, as well as the viscous and inviscid flow fields. The most frequently occurring situation involves separation of a turbulent boundary layer. Therefore, data on this type of flow provides a valuable test case for turbulent flow prediction techniques. The sharp changes in pressure gradient in this case serves to test whether a turbulent flow model responds correctly to rapidly changing conditions. In addition to the fundamental problem, it is also a practical problem for missile and projectile designers where proturbances such as rotating bands of artillery projectiles are introduced for non-aerodynamic reasons.

Some of the existing information on the rotating band problem for artillery shell has been summerized in Reference 1 and 2. Young and Patterson[3] have reviewed existing data on aircraft excrescence drag. An important fundamental paper on two-dimensional separated flow is that of Chapman, et al.[4] The present work extends their experimental data to that of axisymmetric geometry and concentrates on the conditions produced by proturbances which are of the same order or smaller than the boundary layer thickness.

This project was initiated as a student project by K. L. Palko and the Mach Number 2.25 data presented here are from that work.[5]

II. EXPERIMENT

The following section describes the details of the experimental procedure and the data reduction technique employed.

1. WIND TUNNEL MODEL

The model used in these tests was made at the University of Delaware. It consists of an aluminum cone of 13.1° half angle, followed by a brass circular cylinder as shown in Figure 1. Five pressure orifices were provided on the model located as shown in the figure. Copper tubing, 0.762mm id with 0.381mm wall thickness, were soldered to the cylinder. Plastic tubing connected the

copper tubing in the model with the scanivalve outside the wind tunnel by passing through the sting and model support.

A transition trip ring of 0.381mm diameter wire was installed on the nose 2.54cm from the tip.

A ring to simulate the effect of a rotating band was made of brass with an inside diameter which matched the outside diameter of the cylinder. The band can be positioned at any point on the cylinder from the first wall tap to the base. It is held in place by a set screw 180° around the model from the pressure orifices. In order to provide enough thickness for the threads of the set screw, a key was machined on the inside of the band which moved in a groove on the underside of the cylinder. In order to prevent disturbances originating from the key-way from disturbing the flow on the test surface, the key-way was filled with wax after setting of the band. Even with these precautions weak waves can be seen in schlieren photographs coming from the imperfect wax surface but none of these waves can be seen on the top of the cylinder where the pressures were measured.

One concern is the possibility that the high pressure ahead of the band could force air under the band and into the low pressure separated region behind. Wax was carefully worked into the cylinder-band junction either ahead or behind the band depending on whether the pressure ahead or behind was of primary interest for that run. Comparison of results with and without this procedure showed no effect of the seal.

After completion of the movable band tests, the brass band was removed and a series of tests using a metal tape band of various thicknesses was undertaken. The tape used consists of 0.127mm thickness, commercial aluminum tape with an adhesive backing. The primary series of experiments involved band widths of approximately 2.2cm, located so that the leading edge of the tape was located at the trailing edge of tap 3 and the trailing edge of the tape was at the leading edge of tap 4. By increasing the number of layers of tape, band thicknesses in the range of 0.127 to 1.143mm were achieved.

2. WIND TUNNEL

The experiments were performed in the U.S. Army Chemical Research Development and Engineering Center's supersonic wind tunnel. This is a movable block, asymmetric nozzle, blow down facility with a capability in Mach number from 1.7 to 3.5. The lower limit in Mach number for these tests of 2.25 was dictated by the model length and reflected shock waves from the tunnel walls. The test section is 15.24cm x 15.24cm in cross section and 45.72cm in length.

3. INSTRUMENTION

The model wall static pressures and the tunnel wall pressures were measured using a diaphragm-strain gauge transducer with a range of ± 172 kPa. The reference pressure was atmospheric. A 48 port Scanivalve sampled each of the six static pressures at a rate of 0.5 seconds per point. The output of the transducer was recorded on a three channel strip chart recorder calibrated to give a linear sensitivity of 0.69 kPa per chart division. The resulting reading accuracy of the static pressures is estimated as ± 0.14 kPa.

The tunnel stagnation pressure was monitored with another strain-gauge transducer with a range of 0 to 1380 kPa gauge referenced to atmospheric pressure. The output was also recorded on a channel of the strip-chart recorder. The output of the transducer was calibrated against a standard test gauge. The recorder sensitivity was set at 27.6 kPa/division for the Mach number 3.00 and 3.50 runs where the nominal stagnation pressures were 620 and 900 kPa gauge respectively. A sensitivity of 13.8 kPa/division was used for the Mach number 2.50 case (Pt = 410 kPa gauge). The reading accuracy of the stagnation pressure was approximately $\pm$ 3.5 kPa. The stagnation pressure varied continuously during each run, particularly following the start of the tunnel. Data were read only after the initial transient had decayed.

The simultaneous recording of the static pressures and stagnation pressure on the same recorder permitted determining a stagnation pressure for each static pressure measurement and these simultaneous readings were used in the data reduction.

Of considerable concern was the measurement of the rotating band position. The technique employed consisted of inserting a 0.762mm diameter drill bit into the pressure tap of primary interest and using machinest gauge blocks between the drill and the band to set the position to within $\pm$ 0.025mm.

4. DATA REDUCTION

The data described here were obtained in a two dimensional movable block wind tunnel. The Mach number in such a facility is easily changed by translation of the lower nozzle block so as to reduce or increase the throat area. The problem with this kind of wind tunnel is that it is difficult to insure that the Mach number is exactly the same from run to run. Experience indicates that the Mach number repeatability is within approximately one to two per cent in this tunnel. This is only a particular problem when the difference of pressure coefficients are taken between different runs.

To compensate for the variation in Mach number, M_∞, the tunnel wall pressure, Pws , was monitored for each run. The tunnel wall pressure port was located ahead of and in a region unaffected by the model. The wall static pressure, however, did not read the correct free-stream static pressure. The measurements showed a consistent 4 to 5 percent higher pressure. Thus the changes in wall static pressure were used to indicate the change in nominal Mach number rather than use it to determine Mach number directly.

The calibrated nozzle block positioning system was employed to set a nominal Mach number, Mn. It was assumed that the average of the ratio of wall static to stagnation pressure, $\langle Pws/Pt \rangle$, from all the same nominal Mach number runs corresponds to nominal Mach number, that is, the variation in actual Mach number, M_∞, from run to run is random. Thus M_∞ for each individual run is determined from:

$$M_\infty = Mn + K[\langle Pws/Pt \rangle - Pws/Pt] \qquad (1)$$

where K is:

$$K = \partial M_\infty / \partial (P_\infty / Pt) \tag{2}$$

and is evaluated using isentropic formulas.

The difference in Cp from two different runs can be correctly formed only if the Mach numbers of the two cases are the same. If the Cp's are significantly different, the small variation in M_∞ produces correspondingly small scatter in the results but when the Cp's are nearly identical (as they are at large distances from the band) the difference in M_∞ produces systematic deviations of the data from zero. To reduce this problem the ΔCp's are calculated using:

$$\Delta Cp = Cp - Cpo = (Pw - Pwo)/(0.5\gamma P_\infty M_\infty^2) \tag{3}$$

where Pw, P_∞, and M_∞ are the wall pressure, free-stream static pressure and test Mach number respectively. P_∞ is evaluated from the measured stagnation pressure and M_∞ so that:

$$\Delta Cp = \frac{\frac{P_w}{P_t}\left[1 + \frac{\gamma-1}{2} M_\infty^2\right]^{\frac{\gamma}{\gamma-1}} - \frac{Pwo}{P_t}\left[1 + \frac{\gamma-1}{2} M_\infty^2\right]^{\frac{\gamma}{\gamma-1}}}{\frac{\gamma}{2} M_\infty^2} . \tag{4}$$

The no-band P'_{wo} was obtained at a different Mach number M′ and its value was adjusted to correspond to M_∞. This is done by assuming that the wall static pressure on the cylinder without the band is essentially the tunnel static pressure so that:

$$\frac{Pwo}{Pt} = \frac{P'_{wo}}{Pt}\left[\frac{1 + \frac{\gamma-1}{2}(M')^2}{1 + \frac{\gamma-1}{2} M_\infty^2}\right]^{\frac{\gamma}{\gamma-1}} . \tag{5}$$

Finally the Cp is calculated from the following equation:

$$\Delta Cp = \frac{\frac{P_w}{P_t}\left[1 + \frac{\gamma-1}{2} M_\infty^2\right]^{\frac{\gamma}{\gamma-1}} - \frac{P'_{wo}}{P_t}\left[1 + \frac{\gamma-1}{2} (M')^2\right]^{\frac{\gamma}{\gamma-1}}}{\frac{\gamma}{2} M_\infty^2} \quad . \qquad (6)$$

III. RESULTS

In the following discussion of results, six aspects of the experiment will be described: A. comparison of the pressure distributions obtained without the rotating band with a Parabolized Navier-Stokes code prediction, B. the validity of the movable band hypothesis will be discussed, C. The effects of Mach number on the perturbations to the pressure distribution caused by the band are considered, D. a general correlation of the pressure distribution is evaluated, E. the effect of band height is evaluated based on the tape band tests, F. an estimate of the band drag coefficient is made.

1. PRESSURE DISTRIBUTION WITHOUT BAND

Measured and predicted pressure coefficients are shown in figures 2a-c for the three nominal Mach numbers, Mn = 2.50, 3.00, 3.50. The solid lines in these figures represent Parabolized Navier-Stokes calculations for the same flow conditions. In each case the data are in good agreement with the predictions, particularly at the higher Mach numbers. The slight discrepancy is of the order of 2% of the dynamic pressure which in the case of the Mn = 2.50 data corresponds to a maximum difference in static pressure of 9%. This departure from the predicted pressure is due to pressure waves generated by the imperfect surface of an access port in the roof of the wind tunnel. This observed deviation was repeatable below Mn = 3.

The pressure coefficients for the cases without the band, Cpo, are listed in Table 1.

TABLE 1. Pressure Coefficients Without Band.

Tap No.	X/D	Mn = 2.25	2.50	3.00	3.50
1	3.895	-0.020	-0.024	-0.020	-0.014
2	4.398	-0.014	-0.010	-0.014	-0.009
3	4.702	-0.012	-0.006	-0.012	-0.007
4	5.598	-0.001	-0.009	-0.002	-0.007
5	5.899	-0.009	-0.004	-0.002	-0.010

The Navier-Stokes code employed is based on the implicit, space marching finite difference algorithm developed by Schiff and Steger.[6] The thin layer equations are in approximate factorization form and use a block tridiagonal technique to obtain the solution. A turbulent boundary layer is calculated

using the Baldwin-Lomax[7] algebraic eddy viscosity model. Because of its space marching formulation it can not be used to predict separated flows. It is one of the objectives of this experiment to provide data with which to validate time dependent Navier-Stokes computations of separated regions currently under development.

2. VALIDITY OF THE MOVABLE BAND HYPOTHESIS

The basic assumption of these experiments is that the pressure change induced by the band depends primarily on the position of the band relative to the pressure tap. On the cylindrical part of the model, where the pressure gradients are small and the boundary layer growth rate is small, the band is expected to cause the same change in pressure, independent of band location. The validity of this idea is shown in Figure 3 and 4 where, for each Mach number tested, the change in pressure coefficient, ΔCp, is plotted versus the relative band position $(X-Xa)/H$.

Each figure contains data obtained from pressure taps 1 through 4. Some of the experiments were performed by locating the leading edge of the band at various distances behind either tap 1, 2 or 3. These data are shown in Figures 3a-c. Similarily the band trailing edge was set at various distances ahead of taps 3 snd 4 to obtain the results shown in Figures 4a-c. The hypothesis is considered valid within the accuracy of the present measuring techniques because all the results at each Mach number accurately form a single curve independent of the tap location used to obtain the data.

3. EFFECT OF MACH NUMBER ON PRESSURE DISTRIBUTION

Figure 5 shows an example of the change in pressure coefficient data obtained from the current experiment at a Mach number of 2.50 plotted against nondimensional position of each tap relative to the leading edge of the band. The maximum ΔCp at the leading edge of the band, Xa, is an estimated point based on extrapolation of the distribution data.

A single observation of the pressures on top of the band is shown in Figure 5 which was actually obtained from the tape band phase of the experiment. The pressure distributions were obtained with the movable metal band of $H/D = 0.040$. No provisions were made for measurement of the pressure on the band itself in these tests. A special single experiment was performed using the tape band ($H/D = 0.0358$) in which the tape covered tap number 2. A hole, punctured through the tape, permitted tap 2 to detect the pressures at one point, $(X-Xa)/H = 0.69$ behind the band leading edge. In each Mach number case, the Cp on top of the band had returned to essentially the Cp obtained without the band. It is concluded that the band width (more than 12 band heights) is so large that the pressure distribution ahead of and behind the band are uneffected by conditions behind and ahead of the band respectively. Although a single observation can not provide conclusive evidence, it suggests that the effects of the expansion from the high pressure on the front face of the band is confined to a very short region on the top of the band near its leading edge.

Of considerable interest is the effect of Mach number on the maximum and minimum ΔCp and the overall size of the interaction region. The maximum and minimum pressures were not measured directly because the pressure orifice

dimensions could not be made arbitrarily small compared to the size of the band. It has been assumed that the measurements represent average pressures over the tap opening. The pressures are plotted in all figures at an X location corresponding to the center of the tap. The highest pressures measured were obtained with the tap half covered by the band (determined by inserting a 0.381mm drill bit into the 0.762mm tap opening and setting the band against the drill bit). The center of the orifice, in this case, is considered to be 0.191mm from the band. The pressure distribution has been extrapolated to X = Xa to obtain ΔCpmax and X = Xb for ΔCpmin.

Table 2 contains the values of ΔCpmax and ΔCpmin determined from the data obtained from these tests and those of Reference 5. Also contained in table 2 are the interaction length La ahead of the band and Lb behind, normalized with respect to the band height, H. La is determined as the distance ahead of the band where the ΔCp is 0.01, i.e., the pressure increase relative to the no band case is one per cent of the dynamic pressure. It is observed that La/H is approximately constant over the Mach number range tested. The average is:

$$La/H = 4.8 \pm 3\% \tag{7}$$

although there seems to be a small but consistent trend toward a decreasing La with increasing Mach number.

The downstream pressure-interaction region is considerably larger and is seen to vary significantly with Mach number. The interaction length Lb is defined in a some what different way because of the extremely gradual pressure recovery. The determination of Lb based on a percentage change in ΔCp would be uncertain because of the small slope of the curves and the scatter in the data. A representative length has been evaluated by drawing straight lines through the data as shown in Figures 4a-c and noting their intersection with the ΔCp = 0 line. The results can be correlated as:

$$Lb/H = 5.4 \times \beta \pm 4\% \tag{8}$$

where:

$$\beta = (M_\infty^2 - 1)^{0.5} . \tag{9}$$

Linearized supersonic flow theory predicts that:

$$\Delta Cp = 2(dy/dx)e/\beta \tag{10}$$

where (dy/dx)e is the effective surface slope. This formula can be used to correlate the present data. An effective body is imagined to replace the recirculation region of the separated flow and any displacement effects of the viscous boundary layer. In the case of the interaction region ahead of the band, (dy/dx)e is assumed to be proportional to H/La, so that:

$$\Delta Cpmax \times \beta = 0.63 \pm 2\% \ . \qquad (11)$$

Behind the band the effective slope is found to be proportional to H/Lb, which in this case is inversely proportional to Beta. Thus:

$$\Delta Cpmin \times \beta^2 = -0.76 \pm 4\%. \qquad (12)$$

TABLE 2. Pressure Distribution Parameters.

Mn	2.25	2.50	3.00	3.50	
ΔCpmax	0.312	0.280	0.220	0.188	
ΔCpmin	-0.194	-0.143	-0.095	-0.066	
La/H	4.96	4.87	4.81	4.67	Ave = 4.8 ± 3%
Lb/H	10.2	12.6	14.9	18.4	
Lb/(H×β)	5.1	5.5	5.3	5.5	Ave = 5.4 ± 4%
ΔCpmax×β	0.629	0.641	0.622	0.631	Ave = 0.631 ± 2%
$\Delta Cpmin \times \beta^2$	-0.788	-0.751	-0.760	-0.743	Ave = -0.760 ± 4%
β	2.016	2.291	2.828	3.354	
Re × 10^{-6}	1.02	1.23	1.33	1.42	

4. CORRELATION OF THE OVERALL PRESSURE DISTRIBUTION

The maximum change in pressure coefficient, ΔCpmax, and interaction length, La/H, for the interaction region ahead of the step have been correlated in terms of Mach number and it is of interest to investigate how well the entire interaction pressure distribution is correlated. Figure 6 shows all the present data plotted in terms of ΔCp/ΔCpmax versus (X-Xa)/La. This indicates that the shape of the dividing streamline (an equivalent body for the separated region) is approximately the same for the range of conditions investigated here. Attempts have been made to use the equivalent body concept as a means of estimating projectile pressure distributions and overall aerodynamic characteristics.[1,2]

Behind the band the situation is more complicated and the data plotted in terms of ΔCp/ΔCpmin versus (X-Xb)/Lb in Figure 7 provides a successful but slightly poorer correlation. The flow field can be pictured as consisting of a recirculating flow region immediately behind the band, followed by reattachment and then a gradual recovery to a zero pressure gradient boundary layer. The length scale of the entire interaction region is sensitive to Mach number as has already been described. The minimum pressure coefficient appears to be related to Lb. The reattachment distance characterized by the most significant part of the pressure recovery is also correlated by the much larger overall length scale Lb.

5. EFFECT OF BAND HEIGHT ON MAXIMUM AND MINIMUM PRESSURE COEFFICIENTS

In an attempt to investigate the effect of different band heights on the surface pressures, various layers of adhesive-backed, aluminum tape were wrapped around the model. Tape was placed on the cylindrical section so that pressure tap 3 was at the leading edge of the tape and tap 4 at the trailing edge. The size of the pressure orifices lead to a difficulty in interpreting these results. For example, with a 0.005 inch tape thickness, the centerline of tap 3 was located 0.381mm ahead of the band or 3 band heights. Examination of Figure 6 shows that $\Delta Cpmax$ is 57% larger than the value measured at $(X-Xa)/H = 3$. Since each band height represents a result at a different relative distance in front of the band, it is difficult to compare one data point with another. The data have been adjusted using Figure 6 to give an estimate of $\Delta Cpmax$ corresponding to $(X-Xa) = 0$. No correction has been applied to the data behind the band except for the 0.241mm band because, for the larger bands, ΔCp is essentially constant for $(X-Xb)/H < 2$.

As has already been described, $\Delta Cpmax \times \beta$ and $\Delta Cpmin \times \beta^2$ are independent of Mach number. By plotting the data in that form it is possible to emphasize the effect of band height alone.

A correlation for the present results can be based on linearized supersonic theory. The slope of the equivalent body can be written as follows:

$$(dy/dx)e = (dy/dx)dsl + d\delta^*/dx \qquad (13)$$

where $(dy/dx)dsl$ is the slope of the dividing streamline between the recirculating separated flow and the detached boundary layer. $(d\delta^*/dx)$ is the displacement thickness effect of the detached boundary layer. It is assumed that:

$$(dy/dx)dsl = Ca1(H/La) \qquad (14)$$

and:

$$(d\delta^*/dx) = Ca2(D/La) \; . \qquad (15)$$

Thus:

$$\Delta Cpmax \times \beta = 2(H/La)[Ca1 + Ca2(D/H)] \; . \qquad (16)$$

For the present data which are essentially at constant Reynolds number, Ca1 and Ca2 are taken to be constants, although it is expected that they may be functions of Reynolds number and D/H. The D/H factor in the second term on the right hand side accounts for the main effects of height on the $\Delta Cpmax$. This formulation is presumed valid for conditions where La/H is constant which can be expected to fail if the band becomes very small or very large with respect to the undisturbed boundary layer.

Except for the smallest band height, the data for small values of D/H are well represented by the formula:

$$\Delta Cpmax \times \beta = 2(H/La)[1.94 - 0.0097(D/H)] \quad . \qquad (17)$$

As D/H becomes large, i.e., H goes to zero, the disturbance caused by the band should dissappear. Therefore it appears that the linear variation with D/H should be modified so that ΔCpmax goes to zero in a more asymptotic manner. Since the range of conditions of primary interest in ballistics is for H/D > .01, a simple second order term is added to the second term on the right hand side which can be justified by the present data. The correlation equation can be written:

$$\Delta Cpmax \times \beta = 2(H/La)\{1.94 - 0.0097\ [1 - .002(D/H)](D/H)\} \quad . \qquad (18)$$

Figure 8 shows the results when the above correlation equation is appplied to the present data ahead of the band.

A discrepancy has been found between the metal and the tape band maximum pressures. The tape band results interpolated to D/H = 25.0 case are about 11% higher than the ΔCpmax values obtained using the movable band. It is not clear what caused this difference. It was observed that the forward face of the tape band was considerably rougher than that of the machined band. In building up 8 to 10 layers of tape, it was impossible to maintain each leading edge exactly over the underlying one. It is possible that this roughened surface influenced the location of the stagnation point and the pressure distribution on the front face of the band. The rear edge of the tape band was as equally rough as the front but ΔCpmin was found to be only 6% higher than the metal band. In terms of the difference in pressure ahead of, minus the pressure behind the band, the tape band data are only 5% higher. In the following correlation formulas, the higher tape band data are used to evaluate the unknown constants.

Another set of experimental data on rotating band height effects at supersonic speed is that of Gorney, et al.[8] In his experiment two band height were tested (1.016 and 2.032mm in height on a 57.15mm diameter model) at Mach number 3.02. The Reynolds number in this test was 5.5×10^6. Gorney's data are included in figure 8 and provide conditions for estimating Reynolds number effects on the ΔCpmax and ΔCpmin. Gorney's model is not the same configuration as the present cone-cylinder. His model was a secant-ogive-cylinder but the band had the same shape and was located on the cylinder several calibers from the ogive nose. There was only one pressure tap in the interaction region ahead of the band and one in the interaction region behind the band. the current data on the variation of pressure with distance from the band was used to adjust the measured pressure to that at Xa. Assuming that Cal and Ca2 are functions of Reynolds number raised to some power, the following final form of the correlation equation is obtained as:

$$\Delta Cpmax \times \beta = 2(H/La)[1.8R^{0.17} - 0.009(D/H - 0.002?(D/H)^2)R^{0.55}] \qquad (19)$$

where R = Reynolds number based on diameter times 10^{-6} Note that this equation assumes La/H = 4.8 independent of Mach number and Reynolds number, although the first function, R × 0.17, may reflect a dependency of La on Reynolds number.

The data behind the band were analyzed in the same fashion as that of the data in front and the results are shown in Figure 9. In this case (dy/dx)dsl is taken proportional to H/Lb. The formula obtained, based on fitting the present and Gorney's data, is:

$$\Delta Cpmin \times \beta^2 = -2(H/Lb)[2.4 - 0.01(D/H - 0.002(D/H)^2)R^{0.34}] \quad . \qquad (20)$$

This equation is remarkably similar to that obtained ahead of the band except for the missing Re dependence of the first term on the right hand side. No adjustment was made in Gorney's ΔCpmin to account for the fact that one of the pressure orifices was 3 band heights downstream of the band.

6. ESTIMATE OF THE DRAG COEFFICIENT

The drag on a small annular ring around a body at zero angle of attack can be written as:

$$Db = \pi DH(Pva - Pvb) \qquad (21)$$

where Pva and Pvb are the average pressures on the front and back faces of the band respectively. In coefficient form, this equation becomes:

$$\Delta C_{Db} = 4(H/D)(Cpva - Cpvb) \qquad (22)$$

which is sometimes written as:

$$\Delta C_{Db}/(d-1) = 2(Cpva - Cpvb) \qquad (23)$$

where d is the maximum diameter of the ring in calibers, d = (1+2H/D). In the present experiment, only the pressures on the cylinder ahead of and behind the band were measured so that just an estimate can be made of ΔC_{Db} based on an assumed relationship between the cylindrical surface pressures and those on the faces of the band.

The pressures on the front face of the band are expected to be higher than the maximum pressure on the cylinder. The situation may be pictured in terms of the dividing streamline separating from the cylinder with nearly zero fluid velocity. Viscous forces produced by the outer flow accelerate the fluid on the dividing streamline until the presence of the band is felt. The dividing streamline then reattaches to the front face of the ring, forming a

stagnation region near the top of the band. The pressure decreases down the band and in the upstream direction along the cylinder. This negative gradient provides the driving force for the recirculating flow. Using this assumed picture of the flow, it is concluded that the maximum pressure on the cylinder is a lower bound for the pressures on the ring. Thus, the drag calculated based on using this pressure as the average on the front of the band is a minimum estimate of the contribution from the front of the ring.

Behind the band the dividing streamline separates from the top corner of the band and reattaches on the cylinder several band heights downstream. The reattachment on the cylinder can be seen as a region of rapid increase in pressure coefficient. A relatively small increase in pressure on the rear face of the band drives the flow as it approaches the separation point on the top of the band. Evidence for this is the relatively constant pressure coefficient immediately behind the band. Thus it is concluded that the minimum pressure on the cylinder is probably a good estimate of the average pressure on the rear face of the band.

The minimum estimate of the band drag coefficient has been calculated based on the the above assumptions and using the correlation equations for the maximum and minimum pressure coefficients. The results, as a function of Mach number, for a typical artillery shell at sea level conditions are shown in Table 3.

TABLE 3. Band Drag Coefficient 155mm Projectile.

M	R	$\Delta C_{Db}/(d-1)$	ΔC_{Db}	$\Delta C_{Db}/C_D$ (%)
1.5	5.15	2.63	0.068	23
2.0	6.88	1.37	0.036	14.
2.5	8.59	0.88	0.023	10.
3.0	10.31	0.61	0.016	7.6
3.5	12.03	0.43	0.011	5.5

Band height = 0.013 cal.
Sea level atmospheric conditions
C_D Based on Reference 9

It is apparent that the contribution from the band increases significantly as the Mach number decreases. However, it should be noted that the present correlation equations are based on linearized supersonic theory which predicts that the pressures approach infinity as beta goes to zero. At transonic speeds this Mach number dependence will over predict the drag. Another aspect of the correlation equations which should be considered when evaluating projectile drag is that the results are sensitive to Reynolds number. The Reynolds number dependence has been determined from very sparce data at low Reynolds number compared to the full scale 155mm case. More data are needed to firmly establish the variation with Reynolds number.

An example which better matches the Reynolds number conditions of the equations is that of a 20mm projectile. The calculated results are shown in Table 4.

TABLE 4. Band Drag Coefficient 20mm Projectile.

M	R	$\Delta C_{Db}/(d-1)$	ΔC_{Db}	$\Delta C_{Db}/C_D$ (%)
1.5	0.66	3.32	0.086	16.5
2.0	0.89	1.89	0.049	10.6
2.5	1.10	1.34	0.035	8.8
3.0	1.33	1.05	0.027	7.6
3.5	1.555	0.86	0.022	7.0

Band height = 0.013 cal.
Sea level atmospheric conditions
C_D data based on Reference 10

IV. CONCLUSIONS

An experiment has been described in which the surface static pressure distribution on a cone-cylinder model with and without a simulated rotating band have been measured. The measurements were obtained at three Mach numbers (2.5, 3.0, 3.5) and at a Reynolds number of $(1.3\pm.1)\times10^6$. Some results from an earlier test at M = 2.25 have also been included.

In order to increase the resolution of the pressure distribution a movable band was used with just five pressure orifices. It has been shown in these tests that essentially the same ΔCp is obtained at corresponding (X-Xa)/H positions independent of the actual location of the band. Measurement of perturbation effects were made on the cylindrical section of the model where boundary layer growth and pressure gradient effects were small.

The pressure disturbance caused by the band has been found to be correlated in terms of the maximum pressure coefficient, $\Delta Cpmax$, and a length scale, La, ahead of the band and a corresponding set of parameters, $\Delta Cpmin$ and Lb, behind the band. Under these supersonic conditions, linearized supersonic theory is shown to apply ahead of the band; in that $\Delta Cpmax$ is inversely proportional to β (where $\beta = (M^2-1)^{1/2}$. The length scale ahead of the band is found to be La/H = 4.8 independent of Mach number. Behind the band, Lb/H is a function of beta such that $Lb/H = 5.7 \times \beta$. Given this result, linearized theory predicts and the experiment confirms that $\Delta Cpmin$ is inversely proportional to β^2.

A second phase of the experiment concerned measurement of the pressure changes caused by various band thicknesses which were created by wrapping layers of adhesive backed metal tape to the model. The correlations developed

in the first phase of the tests were used to estimate the maximum and minimum pressure coefficients from the tape band results. These data can be correlated to show that:

$$\Delta Cpmax \times \beta = 2(H/La)(Ca1 - Ca2 \times f(D/H))$$

$$\Delta Cpmin \times \beta^2 = 2(H \times \beta/Lb)(Cb1 - Cb2 \times f(D/H))$$

where for $D/H < 100$

$$f(D/H) = (D/H) - 0.002(D/H)\times 2 \ .$$

The additional quantities Ca1, Ca2, Cb1 and Cb2 were evaluated using the present data and data from a higher Reynolds number test of Reference 7 at M = 3.02 and $Re_D = 5.5 \times 10^6$. It has been found that the constants are functions of Reynolds number. Accurate determination of the Reynolds number dependancy requires additional information covering a wider range of data.

An argument is advanced that ΔCpmax determined on the cylinder ahead of the band under predicts the pressure on the forward face of the band but that ΔCpmin is a reasonable estimate for the pressures on the rear face. Thus a drag calculated on the basis of the above correlations is likely to represent a lower bound to the band drag. Such estimates of drag coefficients for the 155mm and 20mm projectiles have been carried out and the results show that in the Mach number range from 2.0 to 3.5, the drag due to a 1.3 per cent thick band varies from 14 to 5.5% for the 155mm shell and from 11 to 7% for the smaller projectile.

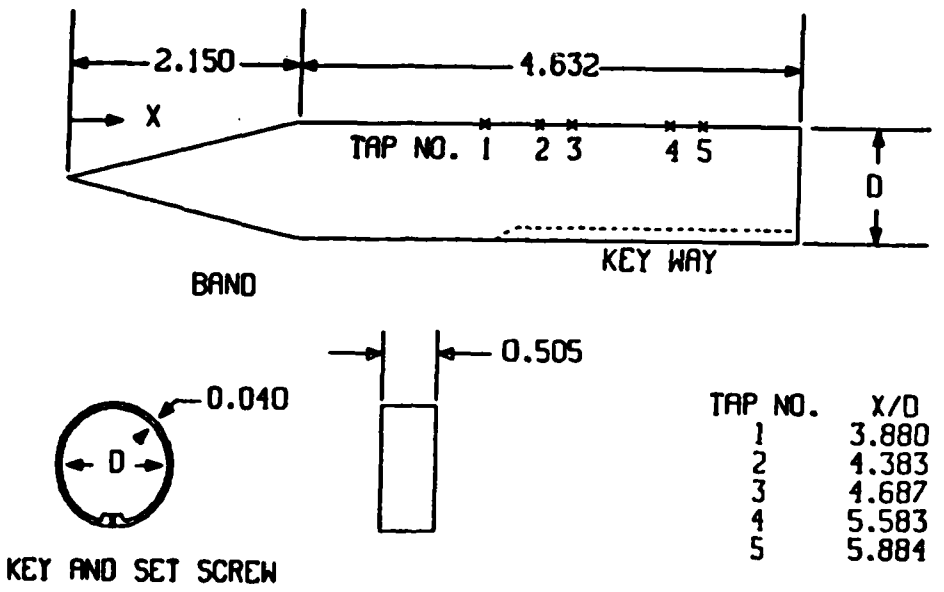

TAP NO.	X/D
1	3.880
2	4.383
3	4.687
4	5.583
5	5.884

ALL DIMENSIONS IN CALIBERS
DIAMETER, D - 2.54 cm

Figure 1. Wind tunnel model.

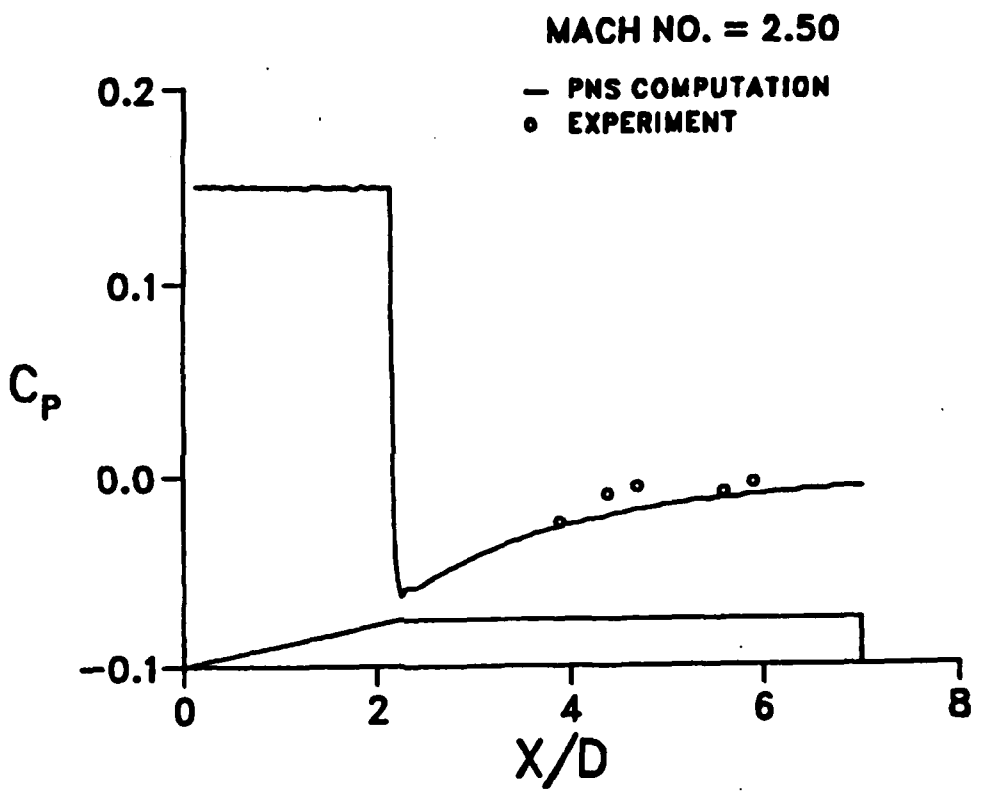

Figure 2a. Pressure coefficient versus position (X/D) without band case, Mach Number = 2.50.

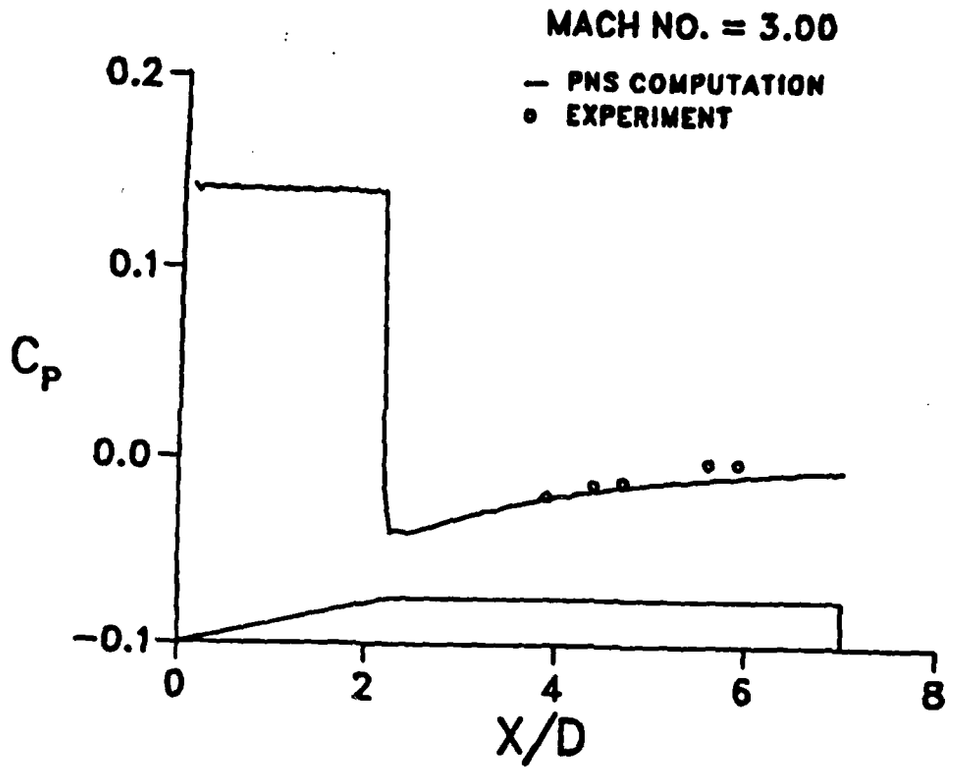

Figure 2b. Pressure coefficient versus position (X/D) without band case, Mach Number = 3.00.

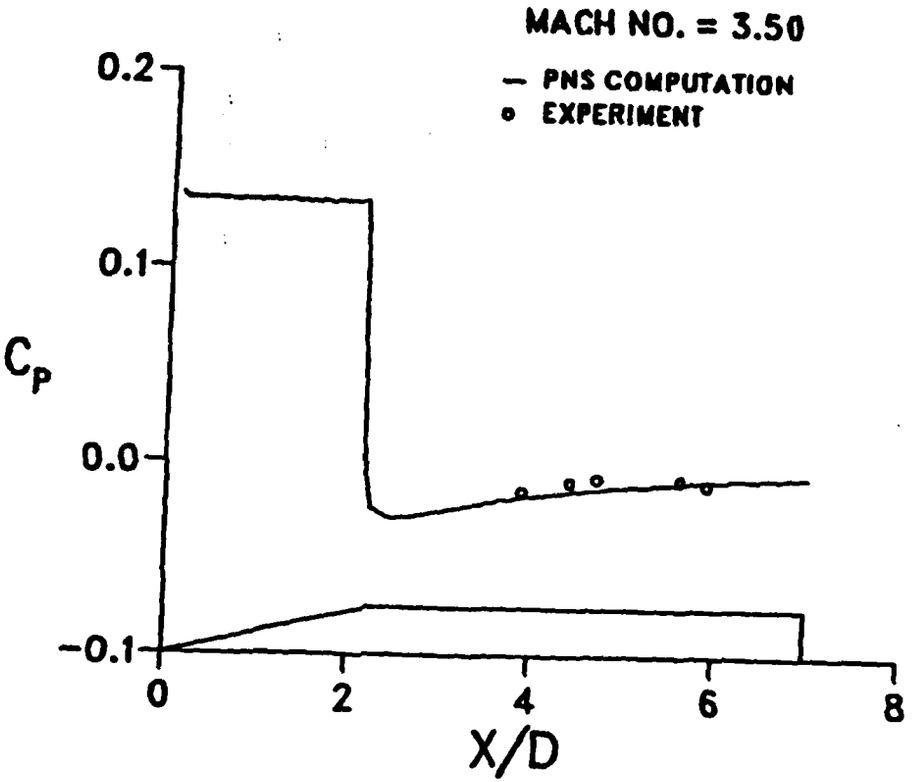

Figure 2c. Pressure coefficient versus position (X/D) without band case, Mach Number = 3.50.

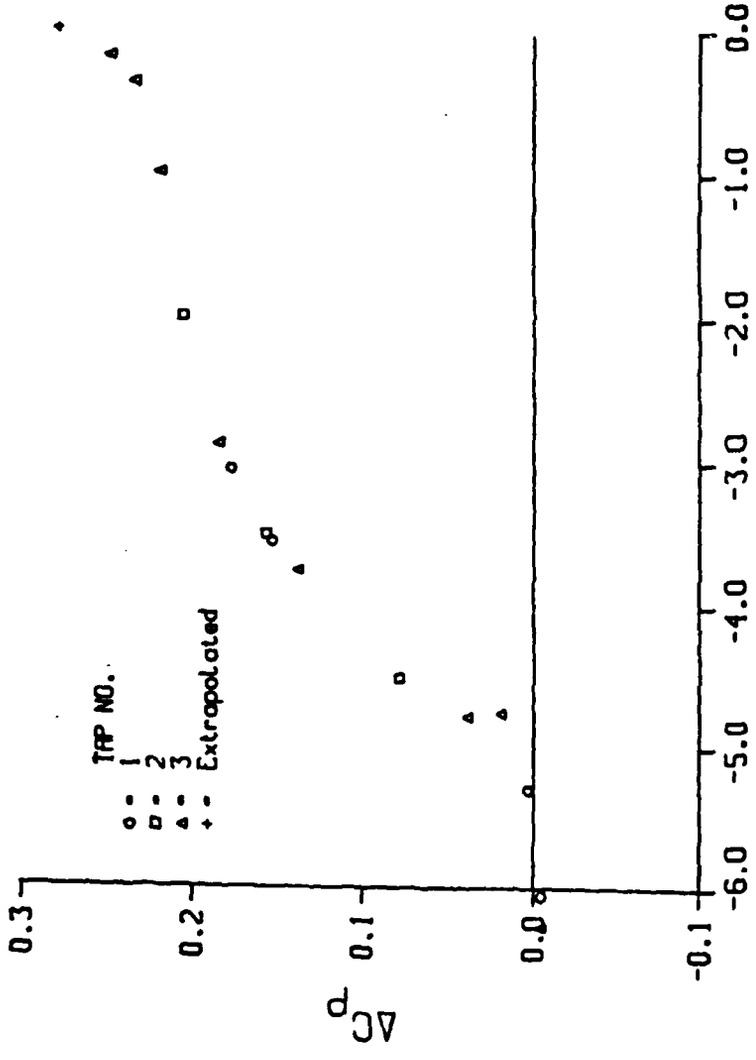

Figure 3a. Cp versus (X-XA)/H ahead of band, Mn = 2.50.

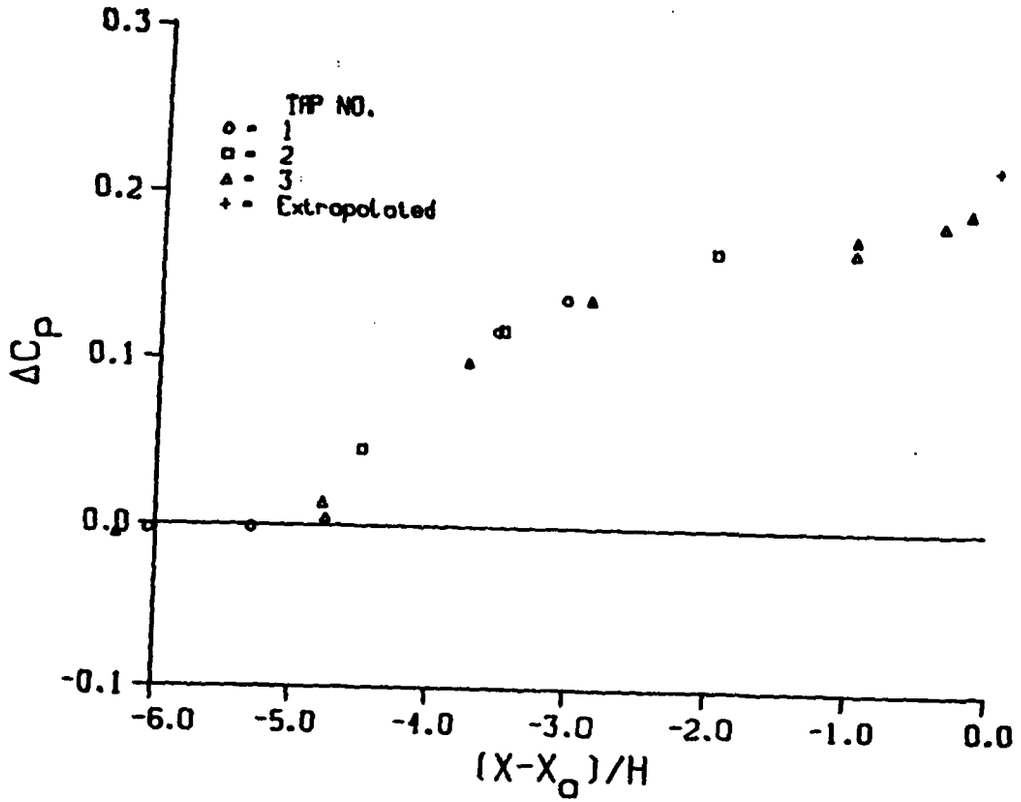

Figure 3b. Cp versus (X-XA)/H ahead of band, Mn = 3.00.

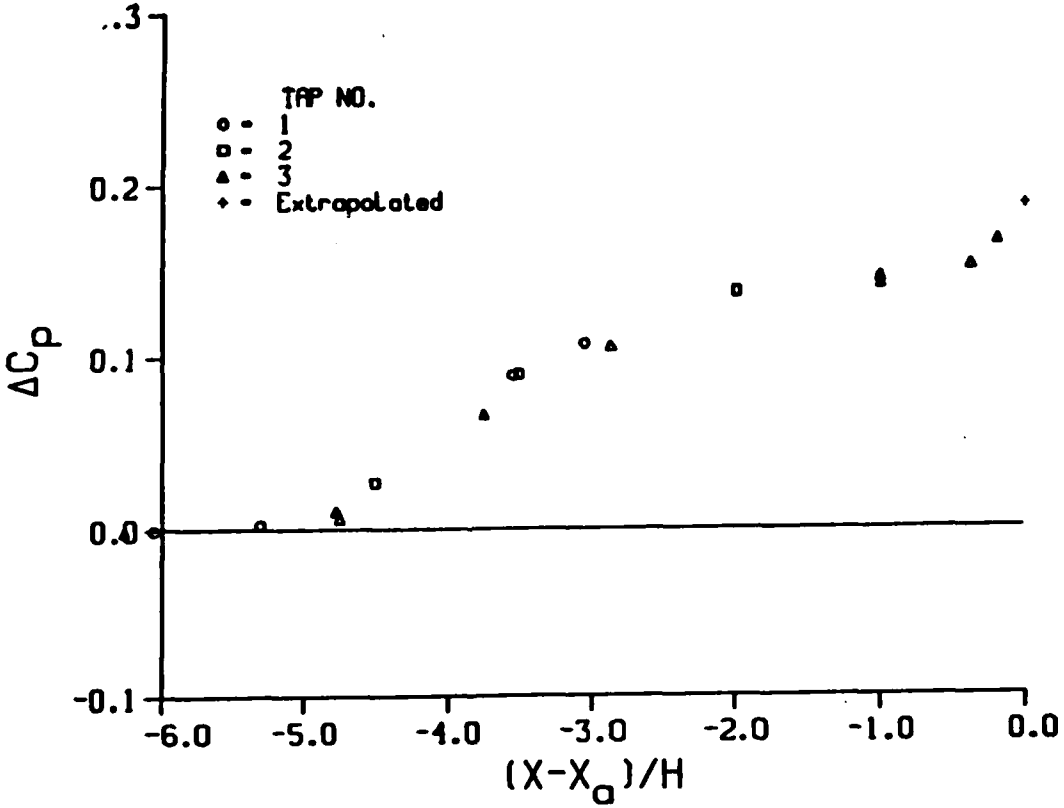

Figure 3c. Cp versus (X-XA)/H ahead of band, Mn = 3.50.

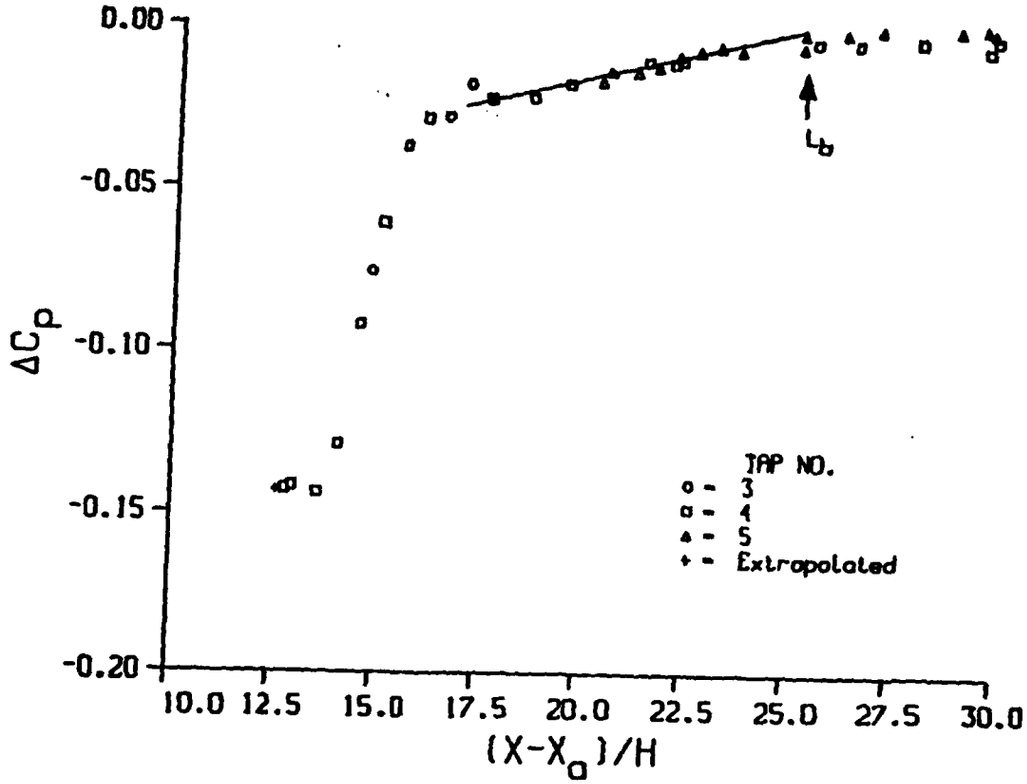

Figure 4a. Cp versus (X-XA)/H behind band, Mn = 2.50.

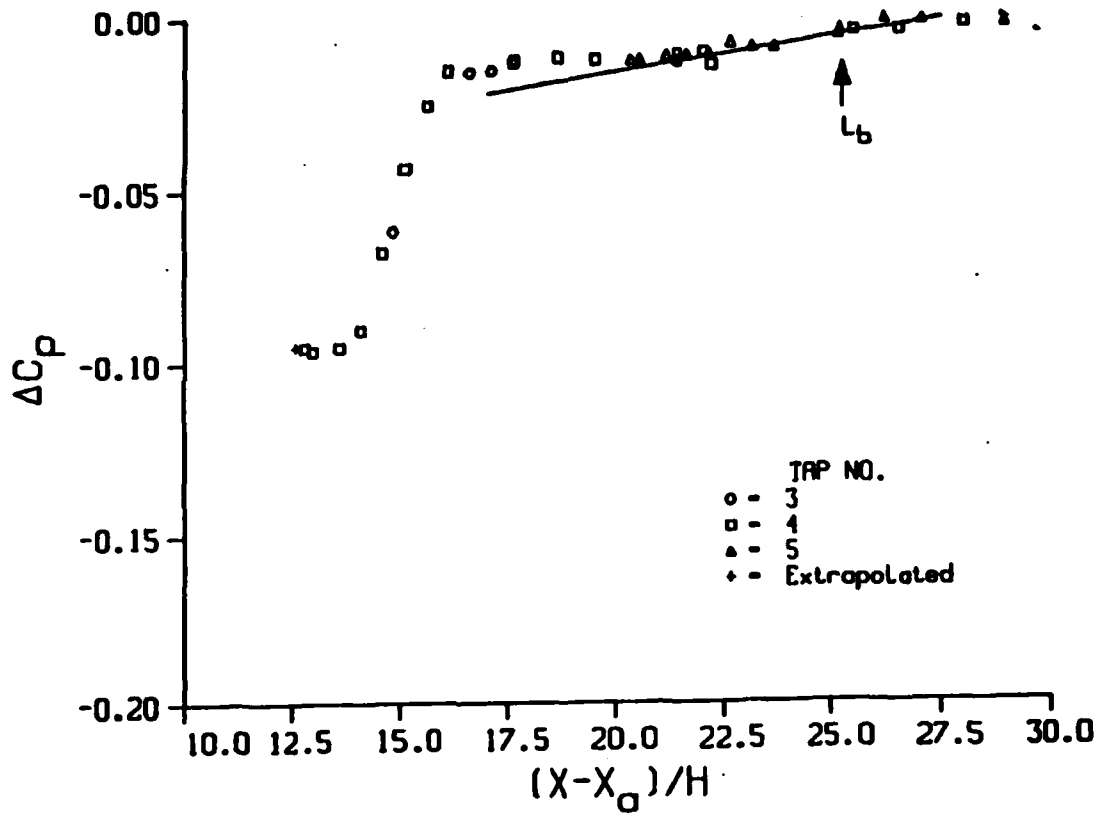

Figure 4b. Cp versus (X-XA)/H behind band, Mn = 3.00.

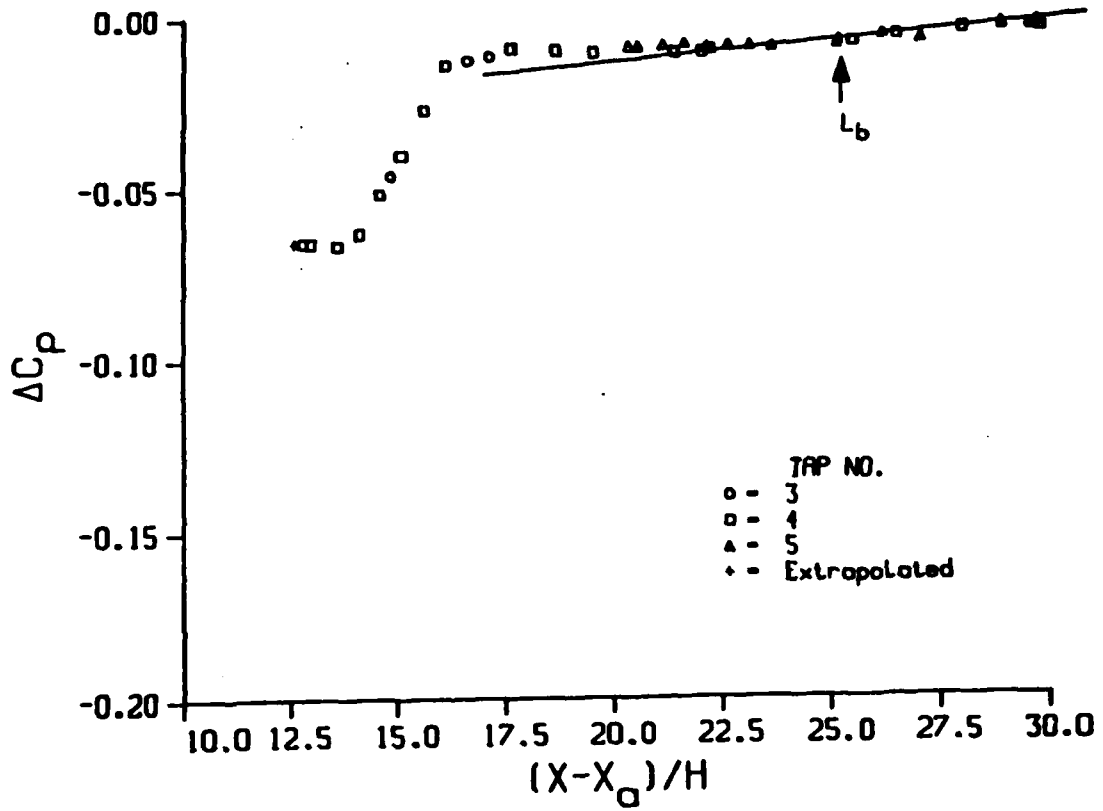

Figure 4c. Cp versus (X-XA)/H behind band, Mn = 3.50.

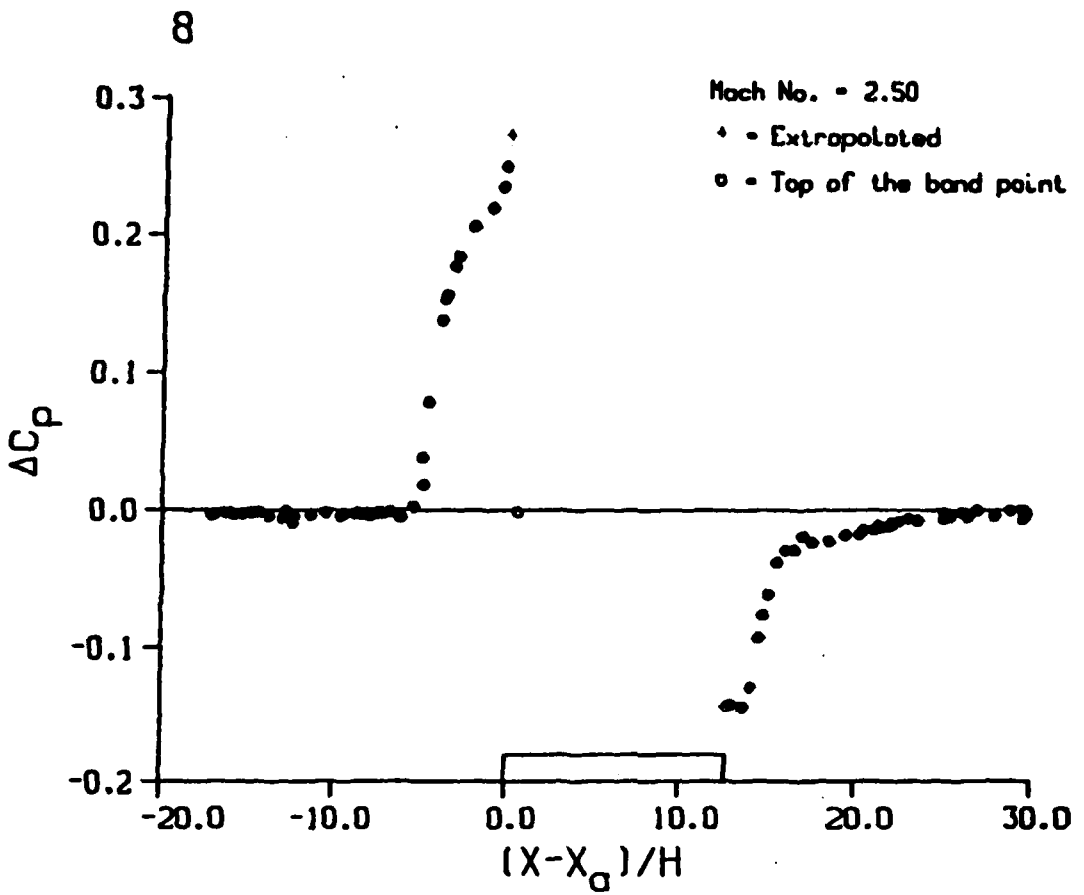

Figure 5. Perturbation pressure distribution (Mach Number = 2.50).

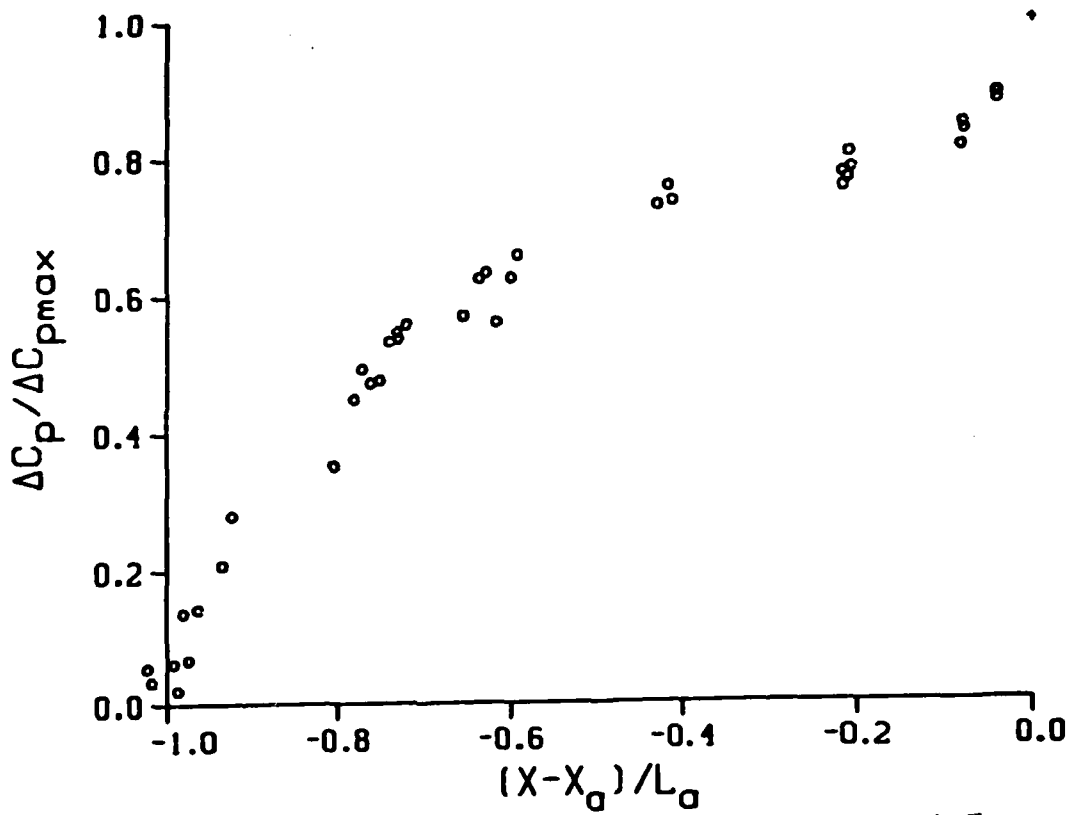

Figure 6. Normalized perturbation pressure distribution ahead of band.

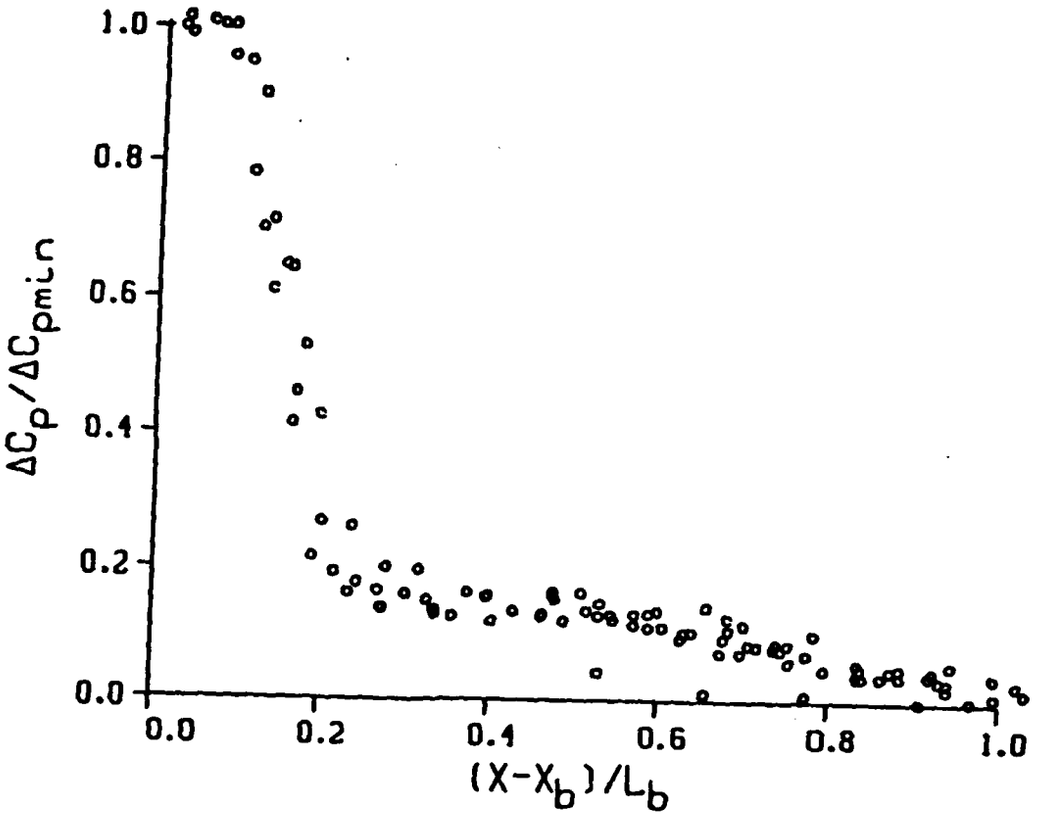

Figure 7. Normalized perturbation pressure distribution behind band.

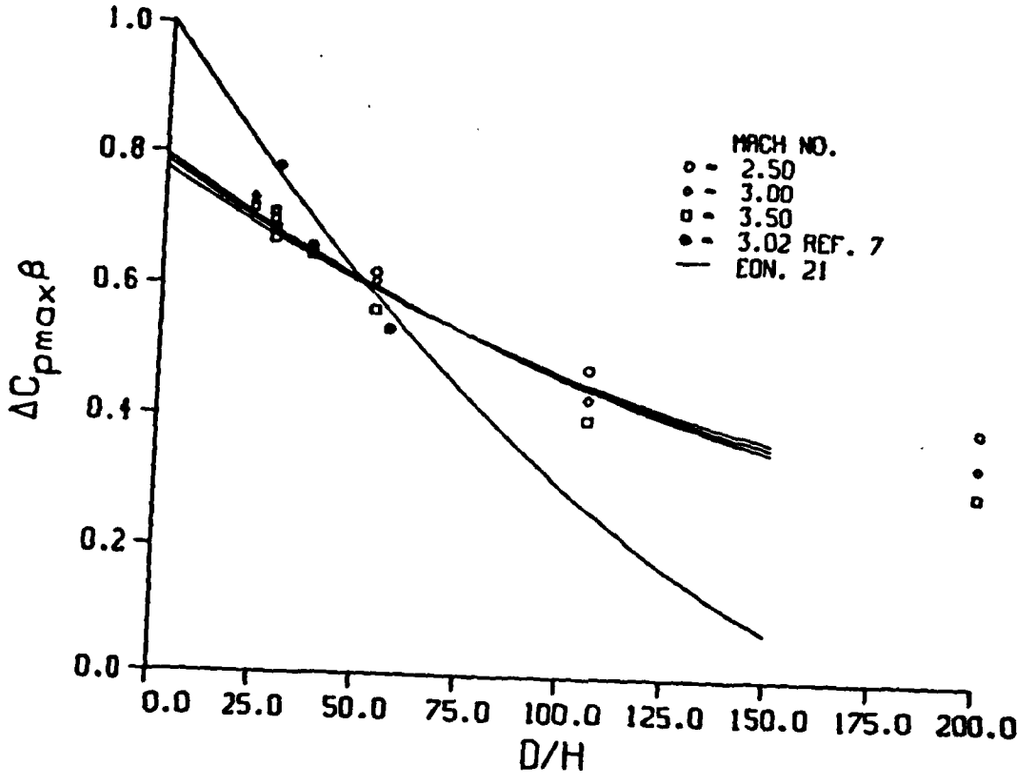

Figure 8. Effect of band height - ahead of band.

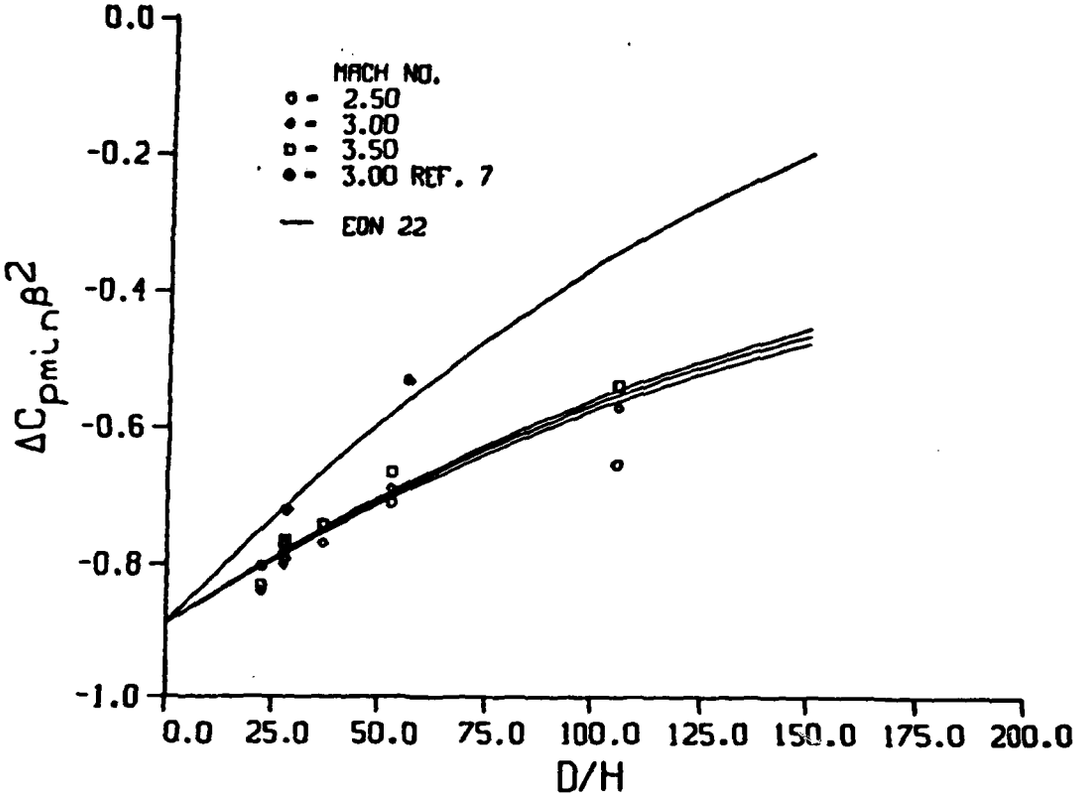

Figure 9. Effect of band height - behind band.

REFERENCES

1. Danberg, J.E., "Numerical Modeling of Rotating Band Flow Field and Comparison with Experiment," Technical Report ARBRL-TR-02505, U.S. Army Ballistic Research Laboratory, Aberdeen Proving Ground, Maryland, July 1983. (AD A131260)

2. Danberg, J.E., Heavey, K.R., and Miller, M.C., "Computational Simulation of Transonic Flow Over Projectile Rotating Band and Comparison with Experiment," Memorandum Report BRL-MR-3447, U.S. Army Ballistic Research Laboratory, Aberdeen Proving Ground, Maryland, May 1985. (AD A159017)

3. Young, A.D. and Patterson, J.D., "Aircraft Excrescence Drag," AGARDDograph No. 264, July 1981.

4. Chapman, D.R., Kuehn, D.M., and Larson H.K., "Investigation of Separated Flows in Supersonic and Subsonic Streams with Emphasis on the Effect of Transition," NACA TR 1356, Ames Aeronautical Laboratory, Moffett Field, California, 1958.

5. Palko, K.L., "Measurement of Surface Pressures Caused by a Projectile Rotating Band," unpublished, presented at the AIAA Central Atlantic Regional Student Conference, Pennsylvania State University, College Park, Pennsylvania, April 19-20, 1985.

6. Schiff, L.B. and Steger, J.L., "Numerical Simulation of Steady Supersonic Viscous Flow," AIAA Paper 79- 0130, 17th Aerospace Sciences Meeting, New Orleans, LA, January 1979.

7. Baldwin, B.S and Lomax, H. "Thin Layer Approximation and Algebraic Model for Separated Flows," AIAA Paper 78-257, January 1978.

8. Gorney, J.L., Yanta, W.J., and Ausherman, D.W., "Laser Doppler Velocimeter Measurements of the Two-Dimensional Boundary Layers on a Projectile Shape at Mach 3," NSWC MP 82-430, Naval Surface Weapons Center, Silver Spring, Maryland, September 1982. (AD A130014)

9. Kline, R., Herrmann, W.R., and Oskay, V., "A Determination of the Aerodynamic Coefficients of the 155mm, M549 Projectile," Technical Report 4764, Picatinny Arsenal, Dover, New Jersey, November 1974. (AD B002073)

10. McCoy, R.L., "'MC DRAG' - A Computer Program for Estimating the Drag Coefficients of Projectiles," Technical Report ARBRL-TR-02293, US Army Armament Research and Development Command, Ballistic Research Laboratory, Aberdeen Proving Ground, Maryland, September 1982. (AD A098110)

LIST OF SYMBOLS

Ca1, Ca2	=	Coefficients in equation (16)
Cb1, Cb2	=	Coefficients in equation (20)
Cp	=	Pressure Coefficient = $(P-P_\infty)/0.5\rho U^2$
Cpo	=	Pressure Coefficient without the band
D	=	Diameter of the projectile
Db	=	Diameter of the band = D+2H
d	=	Diameter of the band in calibers = 1+2H/D
(dy/dx)dsl	=	Slope of dividing streamline
(dy/dx)e	=	Slope of equivalent body
H	=	Height of band
K	=	Factor in equation (2)
La	=	Pressure interaction length ahead of the band
Lb	=	Pressure interaction length behind band
M	=	Mach number
P	=	Pressure
R	=	$Re\times10^{-6}$ (see equation (19))
Re	=	Reynolds number based on projectile diameter
U	=	Free-stream velocity
X	=	Position on projectile measured from the tip
Xa	=	Position of the leading edge of the band
Xb	=	Position of the trailing edge of band

Greek Symbols

β	=	Mach number parameter = $(M^2-1)^{1/2}$
δ^*	=	Boundary layer displacement thickness
ΔCp	=	Perturbation pressure coefficient = Cp - Cpo

ΔC_{pmax}	=	Maximum Cp ahead of the band
ΔC_{pmin}	=	Minimum Cp behind band
ΔC_{Db}	=	Drag coefficient due to the band
γ	=	Ratio of specific heats
ρ	=	Free-stream density

Subscripts

a	=	Ahead of band
b	=	Behind band
n	=	Nominal wind tunnel conditions
o	=	Without KBband
t	=	Wind tunnel stagnation conditions
va	=	Average, front face of band
vb	=	Average, rear face of band
w	=	Model wall conditions
wo	=	Model wall conditions without band
ws	=	Wind tunnel wall conditions Free-stream

DISTRIBUTION LIST

No. of Copies	Organization
12	Administrator Defense Technical Info Center ATTN: DTIC-DDA Cameron Station Alexandria, VA 22304-6145
1	HQDA DAMA-ART-M Washington, DC 20310
1	Commander US Army Materiel Command ATTN: AMCDRA-ST 5001 Eisenhower Avenue Alexandria, VA 22333-0001
8	Commander Armament RD&E Center US Army AMCCOM ATTN: SMCAR-TDC SMCAR-TSS SMCAR-LCA-F Mr. D. Mertz Mr. E. Falkowski Mr. A. Loeb Mr. R. Kline Mr. S. Kahn Mr. H. Hudgins Dover, NJ 07801-5001
1	Commander US Army Armament, Munitions and Chemical Command ATTN: AMSMC-LEP-L Rock Island, IL 61299
1	Director Benet Weapons Laboratory Armament RD&E Center US Army AMCCOM ATTN: SMCAR-LCB-TL Watervliet, NY 12189
1	Commander US Army Armament, Munitions and Chemical Command ATTN: SMCAR-ESP-L Rock Island, IL 61299

No. of Copies	Organization
1	Commander US Army Aviation Research and Development Command ATTN: AMSAV-E 4300 Goodfellow Blvd St. Louis, MO 63120
1	Director US Army Air Mobility Research and Development Command Ames Research Center Moffett Field, CA 94035
1	Commander US Army Communications - Electronics Command ATTN: AMSEL-ED Fort Monmouth, NJ 07703
1	Commander ERADCOM Technical Library ATTN: DELSD-L (Reports Section) Fort Monmouth, NJ 07703-5301
3	Commander US Army Missile Command Research, Development & Engineering Center ATTN: AMSMI-RD Dr. Bill Walker Mr. R. Deep Redstone Arsenal, AL 35898
1	Director US Army Missile & Space Intelligence Center ATTN: AIAMS-YDL Redstone Arsenal, AL 35898-5000
1	Commander US Army Tank Automotive Command ATTN: AMSTA-TSL Warren, MI 48397-5000
1	Director US Army TRADOC Systems Analysis Activity ATTN: ATAA-SL White Sands Missile Range, NM 88002

DISTRIBUTION LIST

No. of Copies	Organization
1	Commander US Army Research Office P. O. Box 12211 Research Triangle Park, NC 27709
1	Commander US Naval Air Systems Command ATTN: AIR-604 Washington, DC 20360
2	Commander David W. Taylor Naval Ship Research and Development Center ATTN: Dr. S. de los Santos Mr. Stanley Gottlieb Bethesda, Maryland 20084
2	Commander US Naval Surface Weapons Center ATTN: Dr. T. Clare, Code DK20 Dr. F. Moore Dahlgren, VA 22448-5000
1	Commander US Naval Surface Weapons Center ATTN: Dr. U. Jettmar Silver Spring, MD 20902-5000
1	Commander US Naval Weapons Center ATTN: Code 3431, Tech Lib China Lake, CA 93555
1	Commander US Army Development and Employment Agency ATTN: MODE-TED-SAB Fort Lewis, WA 98433
1	Director NASA Langley Research Center ATTN: NS-185, Tech Lib Langley Station Hampton, VA 23365
2	Commandant US Army Infantry School ATTN: ATSH-CD-CSO-OR Fort Benning, GA 31905
1	AFWL/SUL Kirtland AFB, NM 87117
1	Air Force Armament Laboratory ATTN: AFATL/DLODL Eglin AFB, FL 32542-5000
3	Sandia Laboratories ATTN: Technical Staff, Dr. W.L. Oberkampf Aeroballistics Division Dr. F. Blottner Albuquerque, NM 87184
3	Director NASA Ames Research Center ATTN: MS-227-8, L. Schiff MS-202A-14, D. Chaussee M. Rai Moffett Field, CA 94035
1	Massachusetts Institute of Technology ATTN: Tech Library 77 Massachusetts Avenue Cambridge, MA 02139
1	Virginia Polytechnic Institute & State University ATTN: Dr. Clark H. Lewis Department of Aerospace & Ocean Engineering Blacksburg, VA 24061
1	University of Delaware Mechanical and Aerospace Engineering Department ATTN: K. L. Palko Newark, DE 19711

DISTRIBUTION LIST

10 Central Intelligence Agency
Office of Central Reference
Dissemination Branch
Room GE-47 HQS
Washington, DC 20502

Aberdeen Proving Ground

Dir, USAMSAA
ATTN: AMXSY-D
AMXSY-MP, H. Cohen

Cdr, USATECOM
ATTN: AMSTE-TO-F

Cdr, CRDC, AMCCOM,
ATTN: SMCCR-RSP-A
SMCCR-MU
SMCCR-SPS-IL

USER EVALUATION SHEET/CHANGE OF ADDRESS

This Laboratory undertakes a continuing effort to improve the quality of the reports it publishes. Your comments/answers to the items/questions below will aid us in our efforts.

1. BRL Report Number_____ Date of Report_____

2. Date Report Received_____

3. Does this report satisfy a need? (Comment on purpose, related project, or other area of interest for which the report will be used.)_____

4. How specifically, is the report being used? (Information source, design data, procedure, source of ideas, etc.)_____

5. Has the information in this report led to any quantitative savings as far as man-hours or dollars saved, operating costs avoided or efficiencies achieved, etc? If so, please elaborate._____

6. General Comments. What do you think should be changed to improve future reports? (Indicate changes to organization, technical content, format, etc.)

CURRENT ADDRESS

Name

Organization

Address

City, State, Zip

7. If indicating a Change of Address or Address Correction, please provide the New or Correct Address in Block 6 above and the Old or Incorrect address below.

OLD ADDRESS

Name

Organization

Address

City, State, Zip

(Remove this sheet along the perforation, fold as indicated, staple or tape closed, and mail.)

FOLD HERE

Director
U.S. Army Ballistic Research Laboratory
ATTN: SLCBR-DD-T
Aberdeen Proving Ground, MD 21005-5066

NO POSTAGE
NECESSARY
IF MAILED
IN THE
UNITED STATES

OFFICIAL BUSINESS
PENALTY FOR PRIVATE USE, $300

BUSINESS REPLY MAIL
FIRST CLASS PERMIT NO 12062 WASHINGTON, DC
POSTAGE WILL BE PAID BY DEPARTMENT OF THE ARMY

Director
U.S. Army Ballistic Research Laboratory
ATTN: SLCBR-DD-T
Aberdeen Proving Ground, MD 21005-9989

FOLD HERE

END

DATE
FILMED

9-86